Phys. Status Solidi C **7**, No. 3–4, 808–811 (2010) / **DOI** 10.1002/pssc.200982794

physica status solidi c
www.pss-c.com
current topics in solid state physics

Electrical characterization of a-C:H as a dielectric material in metal/insulator/metal structures

C. Zúñiga-I.[*], A. Kosarev, A. Torres-J., P. Rosales-Q., W. Calleja-A., F.J. De la Hidalga-W., and O. Malik

Electronic's Department, National Institute for Astrophysics, Optics, and Electronics, INAOE, P.O. Box. 51 & 216, 72000, Puebla, Mexico

Received 31 July 2009, revised 8 October 2009, accepted 15 October 2009
Published online 8 February 2010

PACS 73.61.Jc, 73.61.Ng, 73.40.Rw, 81.15.Gh

[*] Corresponding author: e-mail czuniga@inaoep.mx, Phone: +52 222 247-0517, Fax: (+52) 222-247-0517
Web: www.inaoep.mx

The fabrication and electrical characterization of Metal-Insulator-Metal (MIM) structures, using a-C:H films as the insulating material, are presented in this work. These PECVD carbon films show a very low dielectric constant and a very high resistivity. The current conduction mechanisms were analyzed before and after the post deposition annealing in pure argon ambient at 400°C. For as-deposited films, the experimental *J-U* curves showed that under low biasing regime ($|U| < 8$ V) the space charge limited current conduction is the main transport mechanism, whereas under higher biasing regime ($|U| > 8$ V)) the current transport is dominated by the Schottky mechanism. For annealed structures, under low and high biasing the ohmic and Schottky mechanisms were identified as the main processes for the electrical transport. Finally, we found that both parameters, the dielectric constant and resistivity, decrease slightly after the thermal annealing.

1 Introduction Since a decade ago, several insulating materials presenting a low dielectric permittivity (K) have been proposed for the back end of line (BOL) technology in order to reduce the crosstalk capacitance and RC delays associated with the inter-metallic levels [1,2]. However, the microelectronics industry has kept its interest in the well established SiO_2 related dielectrics. In order to make attractive this new low K insulating film for the microelectronics industry, several technological issues must be addressed.

In spite of several alternatives, the search for a low cost and reliable low K dielectric has not been finished [3]. PECVD carbon-based materials are proposed here because we have developed a well controlled deposition technique to obtain films with excellent electrical properties such as a very low-K (2.1), a high resistivity (10^{14} Ω-cm), and a high breakdown electric field (~10^6 V/cm) [4]. In order to obtain an effective use of a-C:H films for the fabrication of integrated circuits (IC's), a better understanding of the current transport mechanisms governing their electrical behaviour is required. Several groups have studied the electrical behaviour of different dielectric films using capacitor-like devices, and have identified the current transport mechanisms considering Schottky (S), Pool–Frenkel (P-F), and the Space Charge Limited Conduction (SCLC) [5,6]. These works have also shown that the charge transport mechanisms in the capacitors are influenced by the film growth technique and the fabrication procedure.

The main purpose of this work is to analyze the electrical behaviour of Ti/a-C:H/Ti MIM structures taking into account the effects of the thermal annealing on the charge transport mechanisms. This work also explores the possibilities of using low-K a-C:H films for different applications in Microelectronics, for instance, as the inter-metallic insulator in high density IC's. This can be accomplished because our plasma-enhanced deposited (PECVD) films and titanium electrodes are highly compatible with the IC´s silicon-based technology. In Sec. 2 the fabrication process for obtaining the MIM structures is described. In Sec. 3 the electrical characterization using J-U characteristics is discussed. Finally, the conclusions of this work are presented.

2 Experimental procedure The a-C:H films were deposited using a low-frequency (110 kHz) PECVD system with a 250 Ws RF-power. Methane (CH_4) diluted with hydrogen was the main reactive gas mixture. The hydrogen content of the dilution in the gas phase was set to 25%, the pressure at 1.6 Torr, and the substrate temperature was 350 ºC. Further details of the deposition process and the structure stability of the a-C:H films have been reported in [4,7]. The fabrication procedure of the MIM structure was conducted as follows. First, a 0.6 µm titanium layer was evaporated onto a corning glass substrate, after which a 0.6 µm thick carbon film was deposited, and finally, 0.78×10^{-2} cm^2 titanium dots were evaporated on top of the carbon film. Figure 1 shows a cross section of the final structure. The film thickness was measured using an Alpha Step Tencor instrument. The *J-U* plots were measured using a 6517A Keithley SMU for a 20-100 ºC temperature range in steps of 20 ºC. The isothermal annealing of the MIM structures was conducted at 400 ºC under argon environment for 20 minutes. In order to obtain the K parameter, the capacitance was measured using a Phillips 6303A Automatic RLC bridge.

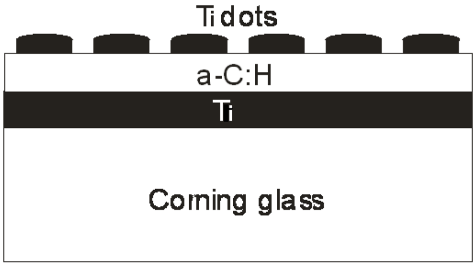

Figure 1 Cross section of the MIM structure.

3. Results and discussion

3.1 *J-U* characteristics at room temperature

The fabrication procedure for these MIM structures matches the BOL technology used in current IC's fabrication processes. For such applications, we are focused on the analysis of the insulating characteristics of the PECVD carbon films. Thus, the S, P-F, and SCLC transport mechanisms proposed to analyze the *J-U* current conduction. Schottky (S), Pool–Frenkel (P-F), and Space Charge Limited Conduction (SCLC) are the well-known transport mechanisms [5,6]. P-F and S current transport models can be described by the following equation:

$$J = J_0 \exp\left[\left(\beta\sqrt{U}\right)/\left(kT\sqrt{d}\right) - e\Phi / kT\right] \quad (1)$$

where J_0 is the saturation current density (which is different for the P-F and the S models), β represents the lowering of the potential barrier, $\beta=\beta_{PF}=2\beta_S=2(e^3/\pi\varepsilon_0 K)^{1/2}$, $\Phi=\Phi_{PF}$ or Φ_S , Φ_{PF} is the trap potential height in the P-F model, Φ_S is the Schottky barrier under a reverse-biasing condition, *k* is the Boltzmann constant, *T* is the absolute temperature, *d* is the thickness of the carbon films, ε_0 is the vacuum permittivity, and K is the dielectric permittivity.

For the SCLC mechanism, the current density can be described as [8]:

$$J=MU^{\gamma} \quad (2)$$

Where *M* and γ depend on the film thickness, trap distribution, and density of states in the amorphous film.

Figure 2 shows the typical *J-U* behaviour of the fabricated MIM structures with Ti electrodes measured at room temperature, and with a biasing voltage varied from -40 to 40 V. Two regions, showing a different slope, can be identified from these curves: a) one for a low applied electric field ($|U|<8$ V), and b) for moderate and higher fields, where the behaviour of the *J-U* curve shows a sharper increase of the electric current.

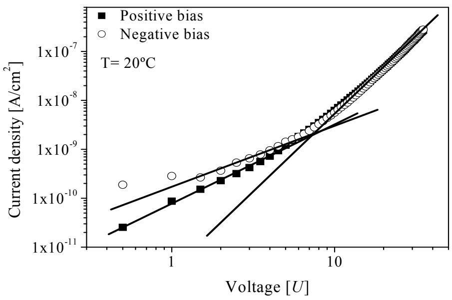

Figure 2 *J-U* characteristics for the MIM structure with Ti electrodes measured at room temperature.

In the low electric field region, the value for the average γ is 1.5, as shown in Fig. 3. It is well known that the typical value for γ is between 1 and 2 for non crystalline materials [8], and in this case it indicates that the SCLC mechanism dominates for low electric fields.

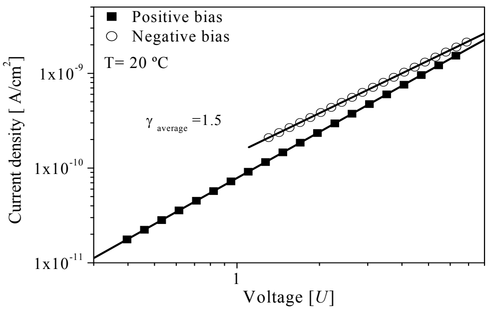

Figure 3 *J-U* characteristics in the low electric field region for the MIM structures with Ti electrodes at room temperature.

In order to identify the main transport mechanism under the applied high electric field, a $\ln(J)$–$U^{1/2}$ curve is plotted, and the current density can be described by

$$\ln(J) = A + B\sqrt{U} \quad (3)$$

Thus, using Eqs. (1) and (3) we can obtain the fitting parameters A and B:

$$A = \left(-e\Phi / kT\right)\ln\left(J_0\right) \quad , \quad B = \beta / kT\sqrt{d} = (1/kT)\sqrt{e^3 / 4\pi\varepsilon_o \mathrm{K} d} \quad (4)$$

Figure 4 shows the ln *(J)*-$U^{1/2}$ curve at room temperature for high electric fields. This behaviour indicates that

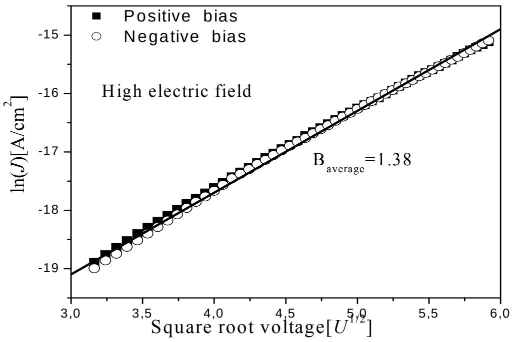

Figure 4 *J-U* characteristics in the high field region for the MIM structures with Ti electrodes at room temperature.

the current transport mechanism could be either Schottky or P-F mechanisms. The fitting of these curves resulted in an average slope ($B_{average}$) of 1.38.

3.2 Influence of the temperature on the *J-U* characteristics The *J-U* measurements were obtained with a ramp voltage from -40 to 40 V, and the temperature was varied from 20 to 100ºC in steps of 20 ºC. As can be seen in Fig. 5, the current density increases monotonically

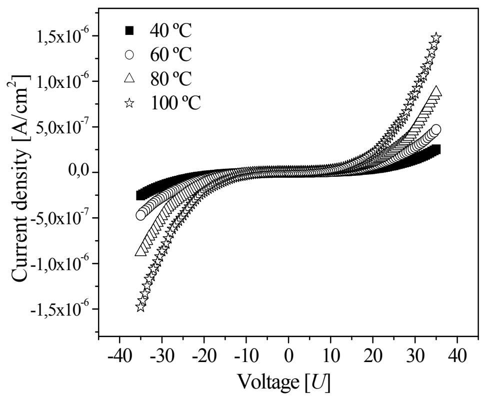

Figure 5 *J-U* characteristics as a function of the temperature.

as the temperature is increased. We can observe that in the range of low electric field (-5 to 5V) the temperature variation does not affect the current density.

The ln *(J)* vs. $U^{1/2}$ curves were also plotted for temperatures of 20 and 100 ºC considering the high electric field region (Fig. 6). For both cases, the *J-U* curves can be described by Eq. (3), with a $B_{average}$ that depends on temperature (B^{JU} = 1.38 and 1.36 for 20 and 100 ºC, respectively). The curves of Fig. 6 are in agreement with both P-F and S mechanisms. The dependence of the curves on temperature allows for identifying the dominant transport mechanism because the S mechanism must depend strongly on the temperature whereas P-F must depend on the applied voltage [9]. The *J-V* curves shown in Fig. 5 can be described by equation (1) and, at first sight, it is difficult to identify the dominance of any transport mechanism. However, we calculated B from equation (4) using the values 2.57 and 2.40 for K, obtained previously from independent measurements of capacitance at 20 and 100°C, respectively (see Table 1). Thus, we obtained B_S^K = 1.33 at 20 °C and 1.10 at 100 °C; and B_{PF}^K = 2.66 at 20 °C and 2.20 at 100 °C. As can be seen, the B_{PF}^K values are closer to those obtained experimentally for B^{JU}, suggesting

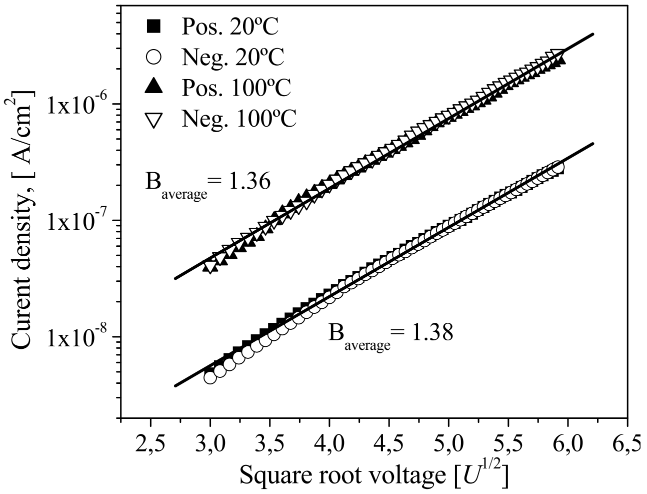

Figure 6 *J-U* characteristics in the high electric field region.

that the Schottky transport mechanism is the dominant in the structures, as it was previously reported for MIS structures [10].

Table 1 Capacitance measurements as a function of the temperature.

T [ºC]	C [pF]	K
20	35.8	2.57
40	34.6	2.50
60	33.9	2.43
80	33.7	2.42
100	33.5	2.40

3.3 Influence of the annealing on the transport properties The MIM structures were annealed at 400 °C, under an argon flow for 30 minutes, and the *J-U* curves were measured. Figure 7 shows a comparison of these curves before and after the thermal treatment, while Fig. 8 shows the same *J-U* curves for the low electric field region. The curves for the annealed MIM structure present a linear relationship, with a calculated slope (γ parameter) of 1.0, which indicates that the ohmic conduction is the dominant mechanism in this region. This mechanism conduction also makes evident that the hopping of electrons from one state to another is present [11]. Figure 9 shows the ln*(J)* vs. $U^{1/2}$ curves, plotted at 20 °C for both samples before and after the thermal annealing. A calculated $B = 1.53$ was obtained from Fig. 8 for the annealed sample. If we compare the previous B value with that calculated using Eq. (4), we obtain $K = 1.95$ using the capacitance value of 27.1 pF at 20 °C, hence $B = 1.51$. These values demonstrated that the S mechanism is dominant, and the transport mechanism is electrode-controlled before and after the thermal annealing. Additionally, we found some variations in the electrical properties of the a-C:H films, as shown in Table 2. The resistivity and the K parameter decreased after the annealing treatment. This work corroborates some of the L.H. Chou´s results [12], where it was shown that the conductivity of carbon PECVD films depends on the sp^2 and sp^3 bonds concentration, which are a consequence of the hydrogen content.

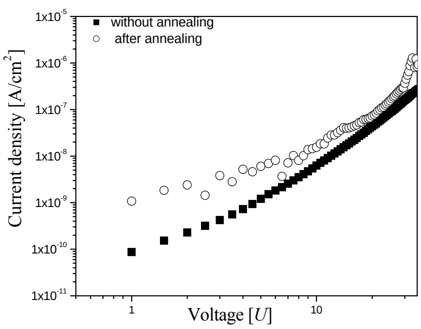

Figure 7 Effect of the annealing on the *J*-*U* characteristics for the low and high electric field regions.

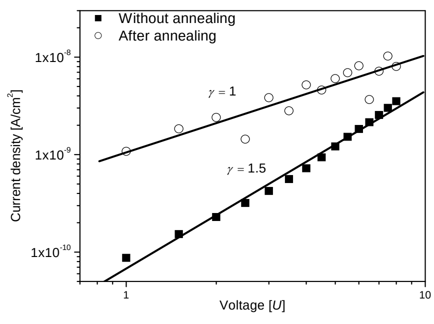

Figure 8 Effect of the annealing on the *J*-*U* characteristics in the low electric field region.

Table 2 Electrical properties of the a-C:H films before and after the thermal annealing.

	K	ρ (Ωcm) at 4 V
As deposited	2.22	1.1×10^{14}
After annealing	1.95	1.9×10^{13}

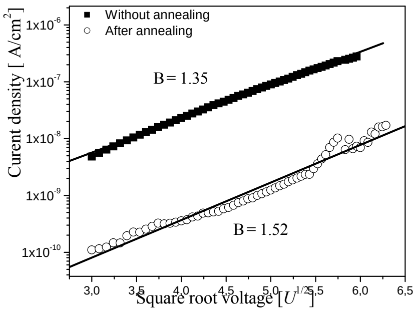

Figure 9 Effect of the annealing on the *J*-*U* characteristics in the high electric field region.

4 Conclusions In this work, we have investigated the transport mechanism in MIM structures with a-C:H as the insulator material before and after a thermal annealing. Before the annealing, the charge transport in the structures can be described as due to SCLC in the low electric field region, and Schottky emission for higher fields. On the other hand, ohmic conduction and Schottky emission determine the transport after the thermal annealing. The current density–voltage measurements indicate that the current transport is bulk-controlled for $|U| > 8$, whereas the conduction is electrode controlled for at $|U| < 8$. The isothermal annealing at 400 °C improved the electrical properties of the film, leading to a significant reduction in K from 2.22 to 1.95, and the resistivity shows a small reduction from 1.1×10^{14} to 1.9×10^{13} Ω-cm. This work explored the possibility of using this low-K a-C:H film for different applications in microelectronics, for example, as intermetallic insulator in high density IC's. It is worth mentioning that the plasma-enhanced deposition (PECVD) technique and the use of titanium electrodes are compatible with the silicon-based IC's technology.

References

[1] S.P. Murarka, Solid State Technol. **3**, 83 (1996).
[2] S.P. Jeng, Mater. Res. Symp. Proc. **337**, 25 (1994).
[3] A. E. Brown, Semic. International, May, 41 (2005).
[4] A. Kosarev, A.Torres, C. Zúñiga, Proc. Nanotechnology, Vol. 3 (2003), pp. 29-32.
[5] S. Gogoi and K. Barua, Thin Solid Films **92**, 227 (1982).
[6] R.D. Gould and B.S.J. Ismail, Mater. Sci. Lett. **11**, 313 (1992).
[7] A. Torres, A. Kosarev, and C. Zúñiga, J. Non-Cryst. Solids **329**, 174 (2003).
[8] Pradip K.R. Kalita, B.K. Sarma, and H. L. Das, Bull. Mater. Sci. **26,** 613 (2003).
[9] S. M. Sze, Physics of Semiconductor Devices, 2nd ed. (New-York Wiley, 1981).
[10] C. Zúñiga, A. Torres, and A. Kosarev, J. Non-Cryst. Solids **338-340**, 326 (2004).
[11] D. Brassard and M. A. El Khakani, J. Appl. Phys. **93**(7), (2003)
[12] L.H. Chou and W. T. Hsih, J. Appl. Phys.**75**(4) (1994).